Validation of a semi-automatic co-registration of MRI scans in patients with brain tumors during treatment follow-up

van der Hoorn, Anouk; Yan, Jiun-Lin; Larkin, Timothy J.; Boonzaier, Natalie R.; Matys, Tomasz; Price, Stephen J.

Published in:
Nmr in biomedicine

DOI:
10.1002/nbm.3538

Publication date:
2016

Validation of a semi-automatic coregistration of MRI scans in brain tumor patients during treatment follow-up

Anouk van der Hoorn, MD PhD[1-3†]; Jiun-Lin Yan, MD[1,4-5†*]; Timothy J Larkin, PhD[1]; Natalie R Boonzaier, MSc[1], Tomasz Matys, MD PhD[2]; Stephen J Price, BSc MBBS(Hons) PhD FRCS(Neuro Surg.)[1]

[†]contributed equally;
[1] Brain tumor imaging lab, Division of neurosurgery, Department of clinical neuroscience, University of Cambridge, Addenbrooke's hospital, Box 167, CB2 0QQ, Cambridge, United Kingdom;
[2] Department of radiology, University of Cambridge, Addenbrooke's hospital, Box 218, CB2 0QQ, Cambridge, United Kingdom;
[3] Department of radiology (EB44), University Medical Centre Groningen, University of Groningen, Box 30.001, 9700 RB, Groningen, The Netherlands;
[4] Department of neurosurgery, Chang Gung Memorial Hospital, 22 Majing road, 204, Keelung, Taiwan
[5] Department of neurosurgery, Chang Gung University College of Medicine, 259 Wenhua 1st road, 333, Taoyuan, Taiwan

Corresponding author:
Jiun-Lin Yan
Division of neurosurgery
Department of Clinical neuroscience
University of Cambridge
Addenbrooke's hospital
Box 167
CB2 0QQ
Cambridge, United Kingdom

Running title: Coregistration of MRI in brain tumor patients
Word count: 4342
Figures: 5
Tables: 2
Supporting material for online-only publication: Yes

ABSTRACT

There is an expanding research interest in high-grade gliomas because of their significant population burden and poor survival despite the extensive standard multimodal treatment. One of the obstacles is the lack of individualized monitoring of tumor characteristics and treatment response before, during and after treatment. We have developed a two-stage semi-automatic method to co-register MRI scans at different time points before and after surgical and adjuvant treatment of high-grade gliomas. This two-stage co-registration includes a linear co-registration of the semi-automatically derived mask of the preoperative contrast-enhancing area or postoperative resection cavity, brain contour and ventricles between different time points. The resulting transformation matrix was then applied in a non-linear manner to co-register conventional contrast-enhanced T1-weighted images. Targeted registration errors were calculated and compared with linear and non-linear co-registered images. Targeted registration errors were smaller for the semi-automatic non-linear co-registration compared with both the non-linear and linear co-registered images. This was further visualized using a three-dimensional structural similarity method. The semi-automatic non-linear co-registration allowed for optimal correction of the variable brain shift at different time points as evaluated by the minimal targeted registration error. This proposed method allows for the accurate evaluation of the treatment response, essential for the growing research area of brain tumor imaging and treatment response evaluation in large sets of patients.

Keywords: Linear coregistration; nonlinear coregistration; brain tumors; high grade gliomas; MRI; treatment response; validation; structure similarity;

Abbreviation:

2D (two-dimensional)

3D (three-dimensional)

FAST (FMRIB's Automated Segmentation Tool)

FLIRT (FMRIB's linear image registration tool)

FMRIB (Oxford center for functional MRI of the brain)

FMRIB Software Library (FSL)

FNIRT (FMRIB's non-linear image registration tool)

MNI (Montreal Neurological Institute)

SAC (Semi-automatic non-linear coregistration)

INTRODUCTION

Despite advances in the treatment of high-grade gliomas, including the introduction of concomitant chemoradiotherapy and adjuvant chemotherapy [1], these tumors continue to carry a high mortality rate and significant population burden [2, 3]. One of the unmet needs in treatment development research is the ability to easily identify differences in tumor characteristics and treatment response with MRI biomarkers before, during and after therapy. This would facilitate research on the treatment response in large sets of patients and the discovery of new imaging biomarkers, further enabling the personalization of therapy. In order to meet this demand, an easily applicable co-registration method is needed to co-register postoperative with preoperative images during the MRI assessment of high-grade gliomas.

A non-linear registration is needed, as brain shift and deformation pose significant challenges when comparing brain MR images at different time points. These changes do not only occur after the initial surgical procedure, but, rather, are a dynamic continuous process [4]. In addition to the structural changes caused by surgery, tumor response to treatment and chronic radiotherapy effects induce further changes. These include, for example, changes in tumor volume [5], making the co-registration process even more difficult.

Although previous research has aimed to address these obstacles, an easily accessible and applicable co-registration method is not yet available for preoperative and postoperative MRI scans of patients with brain tumors. Most methods focus on the co-registration of different sequences of the same scan time point with linear and non-linear registration methods in healthy subjects and patients with brain tumors. These existing methods demonstrate good performances for this intra-subject

co-registration of data from the same time [6, 7] or to a standardized brain atlas [8, 9]. Research has also demonstrated the value of a non-linear co-registration for treatment response evaluation in patients without surgery [10]. However, surgery is part of the standard treatment scheme in patients with high-grade gliomas [1] and is regularly performed in other primary and metastatic brain tumors [11, 12]. Therefore, the ability to deal with post-surgical changes should be part of the co-registration method.

Methods of MRI co-registration taking resection into account are scarce and have several limitations, making them unsuitable as a widely and easily usable co-registration method. The few available clinical studies that have used an intra-subject co-registration method after surgery are difficult to replicate and evaluate as they use in-house software, and provide only limited details of methodology [e.g. refs. [13-15]]. Technical studies suffer from other issues, such as small sample size [16]. Another study has tested methods only on epilepsy patients with whole lobe resection [17], where fewer signal changes and mass effects are expected. Furthermore, these and other technical papers do not provide comprehensible co-registration guidelines, thereby hindering wide applicability, especially for clinical researchers [16-18].

There are a few methods available that co-register intraoperative images with preoperative imaging. However, these are limited by using other modalities, such as computed tomography (CT) [19], tracked laser range scanning [20] or ultrasound [21]. CT is inferior to MRI in detecting tumor recurrence and thus is not routinely used for the treatment evaluation or research of patients with brain tumors. Ultrasound and laser imaging are only possible during surgery when the skull is temporarily removed.

The method of Nithiananthan et al. [19] uses an approach that defines resected voxels based on an air density. This is not applicable to research with interest in tumor response assessment as the resection cavity being filled with fluid and/or adjacent brain tissue rather than air. Other ‘preoperative with intraoperative co-registration’ methods have only tested the complex algorithm on two-dimensional (2D) data [22]

Therefore, there is a need for an easily applicable and usable co-registration method before, during and after treatment, including surgical resection. To address this, we have developed a semi-automatic co-registration technique employing widely used and freely available software. This may allow the accurate evaluation of the treatment response in future studies, which is essential for brain tumor imaging research and treatment response assessment in large sets of patients. We also provide detailed information about the steps and code used.

METHODS

Patient inclusion criteria

Patients with newly diagnosed supratentorial glioblastoma, operated on from 2010 to 2014, were included in the study. Exclusion criteria were previous cranial surgery, previous cerebral radiotherapy or another known primary tumor. We included 32 patients (mean age, 56 years; range, 31–68 years; 20 men) with preoperative MRI scans who also had available follow-up MRI. Follow-up MRI scans included a direct postoperative scan and the scan at the time point of tumor recurrence. Adequate direct postoperative MRI data (<72 h) were available for 30 patients, whereas later follow-up at the time of tumor recurrence was available for 27 patients (mean of 12 months after the operation date; range, 0.8–38 months). All patients were treated with maximal surgical resection, followed by standard concomitant chemoradiotherapy and then by adjuvant chemotherapy [1].

Data acquisition

Preoperative MRI data acquisition was performed using a 3.0-T Siemens Magnetom MRI system (Siemens Healthcare, Munich, Germany) with a standard 12-channel head coil. Imaging included an anatomical three-dimensional (3D) T1-weighted sequence with fat suppression acquired after the intravenous injection of 9 mL of gadolinium (Gadovist, Bayer Schering Pharma, Berlin, Germany) (TR/TE = 900/2.98 ms; inversion time, 900 ms; flip angle, 9°; field of view, 256 × 240 mm^2; 176–208 slices; no slice gap; voxel size, 1 × 1 × 1 mm^3).

Follow-up MRI scans were acquired on a 1.5-T GE Optima, 1.5- or 3.0-T GE Signa (General Electric Company, Little Chalfont, Buckinghamshire, UK) or 1.5-T Siemens Avanto (Siemens Healthcare) with standard head coil. Imaging included a

T1-weighted anatomical sequence after the intravenous injection of 9 mL of gadolinium (Gadovist, Bayer Schering Pharma). This was performed as a 2D T1-weighted sequence (TR/TE = 440–771/8–21 ms; flip angle, 58°–90°; field of view, 220–240 × 207–240 mm^2; 20–85 slices; slice gap, 0–1 mm; voxel size, 0.429–0.7188 × 0.429–0.7188 × 3–6 mm^3), a 2D T1 inversion recovery sequence (TR/TE = 2508–2600/12–42 ms; inversion time, 780–920 ms; flip angle, 90°–110°; field of view, 220 × 220 mm^2; 20–22 slices; slice gap, 1–3.5 mm; voxel size, 0.4297 × 0.4297 × 6 mm^3) or a 3D T1 fat-suppressed sequence (TR/TE = 7/2.948 ms; inversion time, 900 ms; flip angle, 190°; field of view, 256 × 256 mm2; 190 slices; no slice gap; voxel size, 1 × 1 × 1 mm^3).

Coregistration method

Co.-registration was performed using a two-stage semi-automatic method (Fig. 1). Conventional contrast-enhanced T1-weighted images were co-registered using tools from the Oxford Centre for Functional MRI of the Brain (FMRIB) Software Library (FSL) version 5.0.0 (http://fsl.fmrib.ox.ac.uk/fsl/fslwiki/). Before the co-registration stages commenced, all images were realigned with the anterior commissure as the center point (coordinate 0, 0, 0) to minimize the influence of brain position. The first stage was the co-registration of the binary masks, which consisted of the outer contour of the brain, the ventricles and contrast-enhancing area (presurgical MRI images) or resection area (follow-up MRI images). This was performed for each subject at different time points to create a transformation matrix (Fig. 1, step 4, using the FLIRT, FMRIB's Linear Image Registration Tool, function). The brain contours were created from the inversion of the brain masks which were semi-automatically extracted [23]. This was followed by manual correction (Fig. 1, steps 1 and 2) and the resulting mask was binarized. The ventricles were identified with an automatic segmentation using

the FSL FAST (FMRIB's Automated Segmentation Tool) (Fig. 1, step 3) function [24]. The FAST function also allowed a semi-automatic identification of the contrast-enhancing area or resection cavity. The contrast-enhancing area is targeted for resection and is replaced by the resection cavity on the direct postoperative and later follow-up MRI scans. Therefore, this stage of co-registration allowed for optimal correction of variable brain shift and surgery-induced changes at different time points.

The second stage applied the transformation matrix, acquired from the first stage, as input for a non-linear transformation matrix of the brain images (Fig. 1, steps 5 and 6), using the FNIRT, FMRIB's Non-Linear Image Registration Tool, function. The non-linear transformation of the brain images used additional subsampling levels for regularization. This also included the binary masks of the brain contour and ventricles from both the preoperative reference image and the follow-up image. This resulted in a co-registration of the follow-up brain extracted MRI scans with the preoperative brain extracted MRI scans. The steps with accompanying FSL code are illustrated (Fig. 1) and are provided as Supporting information to facilitate use by others. Standard linear co-registration (FLIRT function) and standard FNIRT with default settings were performed separately for comparison using the FLIRT and FNIRT options in FSL.

Validation methods

Validation was performed using a targeted registration error method for the calculation of the error in different directions. Validation in the x and y directions was performed using the septum pellucidum (Fig. 2A) and cerebral aqueduct (Fig. 2B) on the same axial slice. Validation in the y and z directions was performed using the upper anterior boundary of the third ventricle, at the level of the foramen of Monro

(Fig. 2C), on the same coronal slice. The central point of the tumor or cavity was targeted automatically for the calculation of the registration error at the location at which most errors could be expected. Vectors were also calculated for all targets. All targeted registration errors were calculated for the semi-automatic non-linear co-registration (SAC) method and compared with the targeted registration errors for the linear co-registered and standard non-linear co-registered images. Differences were tested with a Wilcoxon signed rank test or paired t-test depending on the normality. Two-sided p values were used.

In addition, a 3D structural similarity map was created [25] using Matlab (MathWorks Inc., Natick, MA, USA). The 3D structural similarity map was created for each subject, comparing the preoperative reference scan with the co-registered follow-up scan. This was performed for scans obtained immediately postoperatively and at tumor recurrence separately. To display group results, the preoperative images were co-registered to standard MNI (Montreal Neurological Institute) space with a non-linear transformation of the brain images including a lesion mask. This was preceded by a linear transformation of a binary mask of the brain exterior and ventricles. A mean structural similarity mask was then created by transforming the structural similarity mask of each patient to standard MNI space. The resection cavity or contrast-enhancing areas were excluded for the mean structural similarity image, as these values are inherently different. One author (J-LY) also visually inspected all the co-registered MRI scans for accuracy.

RESULTS

Targeted registration error

The targeted registration error showed good performance of the co-registration method for the direct postoperative and recurrence images with a clear benefit over the linear co-registration method and standard FNIRT non-linear co-registration method (Tables 1 and 2). In the co-registration of postoperative to preoperative images, in comparison with FLIRT, the SAC method showed a smaller vector deviation of the cerebral aqueduct (1.1 versus 1.6, $p = 0.015$). A smaller deviation was also detected for the septum pallucidum y coordinate and vector (1.3 versus 2.0, $p = 0.029$; 1.8 versus 2.6, $p = 0.021$), as well as the top of the third ventricle y, z coordinate and vector (0.4 versus 2.2, $p < 0.001$; 1.2 versus 1.9, $p = 0.043$; 1.3 versus 3.3, $p < 0.001$). The SAC method also outperformed the default FNIRT co-registration, where there was small deviation between preoperative and postoperative images for most of the coordinates and vectors in the central tumor/cavity point, cerebral aqueduct, septum pellucidum and the third ventricle at the level of the foramen of Monro.

The benefit of this co-registration method can also be seen in the co-registration of recurrence images to preoperative images (Table 2). The target error at the cerebral aqueduct and the roof of the third ventricle at the level of the foramen of Monro was smaller using the SAC method than the linear co-registration and FNIRT co-registration. When using default FNIRT, there was a larger z coordinate deviation at the tumor centroid point. In addition, the linear co-registration failed in three patients, and default FNIRT co-registration failed in two patients, for both the postoperative and recurrence scan, whereas the semi-automatic method was used without problems.

3D structural similarity

The mean 3D structural similarity of all 32 patients showed the relative performance of the co-registration method (Fig. 3), which is also illustrated using a representative subject by contour overlay images (Fig. 4). The peripheral areas, including the frontal and parietal areas, demonstrated the best performance. A good performance was also seen at the periventricular regions. A relatively smaller overlap between the co-registered and reference preoperative scans was seen in the mid-sagittal and central areas, the centrum semiovale and central cerebellum.

An example of this co-registration is shown in Fig. 5. Without appropriate co-registration, one cannot confidently compare the initial postoperative or tumor recurrence images with the pre-operative reference images (Fig. 5A). Although the standard FNIRT co-registration of postoperative MR and recurrence MR images (Fig. 5B) realigned the images in the same space as the reference images, regional torsions (white arrows) were detected at the resection edges. Using the semi-automatic co-registration methods, the co-registered postoperative MR (Fig. 5C, left) and recurrence MR (Fig. 5C, middle) images were able to show the residual contrast-enhanced lesion (yellow contour) and the recurrent area (red contour) in the reference MR image (Fig. 5C).

DISCUSSION

We have developed and validated a two-stage semi-automatic method for the co-registration of preoperative and follow-up MRI scans for both the direct postoperative and tumor recurrence time points (Tables 1, 2 and Fig. 5). The semi-automatic derived mask of the outer brain contour, ventricles and lesion allowed an accurate co-registration despite the brain shift changes and postoperative changes. Therefore, this method is highly applicable for the analysis of large imaging datasets to evaluate treatment response, a growing and clinically important research area. Furthermore, it can be easily reproduced, allowing a wide applicability of the method.

In the standard FNIRT function, an affine transformation is required as a starting estimate of the co-registration. This affine transformation is typically the result of linear FLIRT co-registration between different MR series. However, the deformation at different time points occurs mainly over the peritumoral regions, resection cavities and ventricles. Our approach was to use the transformation affine of these areas with the greatest changes rather than the whole brain images (Fig. 1, step 4). Furthermore, we added an inverted brain mask as an outer frame to our first stage co-registration for the gross spatial position (Fig. 1, steps 2 and 3). This resulting affine was further applied to the normal brain parenchyma with the mask of ventricle and lesion (Fig. 1, step 5) to achieve the optimal co-registration.

To our knowledge, there is a shortage of easily applicable methods allowing the co-registration of preoperative and postoperative imaging in patients with brain tumors. Clinical papers often use in-house software solutions and provide only a partial description of the methodology [e.g. refs. [13-15]]. This hinders reproducibility

and makes the independent evaluation of reliability difficult. Moreover, technical papers are often complex and use only a small number of patient datasets, e.g. up to two patients with brain tumors [16] and up to six patients with epilepsy surgery [17]. We have created an easily reproducible method (see Supporting information for the code) and have tested it in a large (n = 32) population. Previous studies using intraoperative co-registration have shown a clear advantage of non-linear co-registration with high diagnostic and stereotactic accuracy [10, 26]. This supports the results of the postoperative co-registrations from our study.

This two-stage semi-automatic co-registration method can be replicated using FSL, which is a freely available and widely used software package in the neuroimaging research community. We have provided a detailed description of the steps required to recapitulate this approach (see Fig. 1 and Supporting information). This makes this method easily reproducible by others, including clinical researchers, which further supports the rationale of using FSL for our co-registration method. Given the purpose of this study, we have not attempted to validate the co-registration of patients with brain tumors using other software packages. The interpolation of our semi-automatic method to other software packages might be possible, but would require separate validation.

The MR image acquisition parameters in our dataset varied across subjects and time points. In particular, a contrast-enhanced 3D T1-weighted dataset was available for the preoperative scan, but the follow-up images were almost always 2D and obtained with different MRI parameters and scanners from different manufacturers. Another limitation is that this method assumes that the resection cavity is a result of surgical resection of contrast-enhancing tumor only, and that the recurrent tumor arises from

the non-contrast-enhancing surrounding area. However, the resection volume may extend beyond the area of contrast enhancement to include the 'peritumoral region', particularly if the resection is conducted under the fluorescence guidance of 5-aminoleuvulinic acid [27]. Despite these differences, our validation showed that the method worked in all subjects, making it easily applicable in clinical practice.

At a time when adequate imaging biomarkers are being sought to evaluate treatment response, method applicability is of essence for the development of brain tumor research. Overcoming these treatment-induced problems in the co-registration makes our semi-automatic co-registration technique a valuable method to facilitate research in the expanding area of personalized medicine in patients with brain tumors.

CONCLUSION

We have developed a semi-automatic co-registration method for MRI of brain tumors to allow the accurate evaluation of treatment response in further research. We have demonstrated the good performance of this approach using 3D structural similarity and targeted registration error methods. We have also provided a detailed description of the methodology, which uses freely available software, making it reproducible by the neuroimaging community. This is an essential tool for the growing research area of brain tumor imaging and treatment response evaluation in large sets of patients.

ACKNOWLEDGMENTS

This research was funded by a National Institute of Health Clinician Scientist Fellowship (SJP), a Remmert Adriaan Laan Fund (AvdH), a René Vogels Fund (AvdH) and a grant from the Chang Gung Medical Foundation and Chang Gung

Memorial Hospital, Keelung, Taiwan (J-LY). None of the authors have financial of other conflicts of interest related to the work presented in this paper. This paper presents independent research funded by the UK National Institute for Health Research (NIHR). The views expressed are those of the author(s) and are not necessarily those of the UK National Health Service, the UK NIHR or the UK Department of Health.

REFERENCES

1. Roger Stupp, M.D., Warren P. Mason, M.D., Martin J. van den Bent, M.D., Michael Weller, M.D., Barbara Fisher, M.D., Martin J.B. Taphoorn, M.D., Karl Belanger, M.D., Alba A. Brandes, M.D., Christine Marosi, M.D., Ulrich Bogdahn, M.D., Jürgen Curschmann, M.D., Robert C. Janzer, M.D., Samuel K. Ludwin, M.D., Thierry Gorlia, M.Sc., Anouk Allgeier, Ph.D., Denis Lacombe, M.D., J. Gregory Cairncross, M.D., Elizabeth Eisenhauer, M.D., and René O. Mirimanoff, M.D. for the European Organisation for Research and Treatment of Cancer Brain Tumor and Radiotherapy Groups and the National Cancer Institute of Canada Clinical Trials Group. Radiotherapy plus concomitant and adjuvant temozolomide for glioblastoma. *N Engl J Med* 2005; 352: 987-996.
2. Burnet NG, Jefferies SJ, Benson RJ, Hunt DP, Treasure FP. Years of life lost (YLL) from cancer is an important measure of population burden and should be considered when allocating research funds. *J Cancer* 2005; 92: 241-245.
3. Cuddapah VA, Robel S, Watkins S, Sontheimer H. A neurocentric perspective on glioma invasion. *Nat Rev Neurosci* 2014; 15: 455-465.
4. Nabavi A, Black PM, Gering DT, Westin CF, Mehta V, Pergolizzi RS Jr, Ferrant M, Warfield SK, Hata N, Schwartz RB, Wells WM 3rd, Kikinis R, Jolesz FA. Serial Intraoperative MR imaging of brain shift. *Neurosurgery* 2001; 48: 787-797.
5. Shibamoto Y, Baba F, Oda K, Hayashi S, Kokubo M, Ishihara S, Itoh Y, Ogino H, Koizumi M. Incidence of brain atrophy and decline in mini-mental state examination score after whole-brain radiotherapy in patients with brain metastases: A prospective study. *Int J Radiat Oncol Biol Phys* 2008; 72: 1168-1173.

6. Jenkinson M, Bannister P, Brady M, Smith S. Improved optimization for the robust and accurate linear registration and motion correction of brain images. *Neuroimage* 2002; 17: 825-841.
7. Klein A, Andersson J, Ardekani BA, Ashburner J, Avants B, Chiang MC, Christensen GE, Collins DL, Gee J, Hellier P, Song JH, Jenkinson M, Lepage C, Rueckert D, Thompson P, Vercauteren T, Woods RP, Mann JJ, Parsey RV. Evaluation of 14 nonlinear deformation algorithms applied to human brain MRI registration. *Neuroimage* 2009; 46: 786-802.
8. Zacharaki EI, Hogea CS, Shen D, Biros G, Davatzikos C. Non-diffeomorphic registration of brain tumor images by simulating tissue loss and tumor growth. *Neuroimage* 2009; 46: 762-774.
9. Mohamed A, Zacharaki EI, Shen D, Davatzikos C. Deformable registration of brain tumor images via a statistical model of tumor-induced deformation. *Med Image Ana*l 2006; 10: 752-763.
10. Ellingson BM, Cloushesy TF, Lai A, Nghiemphu PL, Pope WB. Nonlinear registration of diffusion-weighted images improves clinical sensitivity of functional diffusion maps in recurrent glioblastoma treated with bevacizumab. *Magn Reson Med* 2012; 67: 237-245.
11. Kaal ECA, Niël CGJH, Vecht CJ. Therapeutic management of brain metastasis. *Lancet Neurol* 2005; 4: 289-298.
12. Whittle IR. Surgery for gliomas. *Curr Opin Neurol* 2002; 15: 663-669.
13. Hiramatsu R, Kawabata S, Furuse M, Miyatake SI, Kuroiwa T. Identification of early and distinct glioblastoma response patterns treated by boron neutron capture therapy not predicted by standard radiographic assessment using functional diffusion map. *Radiat Oncol* 2013; 8: 192.

14. Moffat BA, Chenevert TL, Lawrence TS, Myer CR, Johnson TD, Dong Q, Tsien C, Mukherji S, Quint DJ, Gebarski SS, Robertson PL, Junck LR, Rehemtulla A, Ross BD. Functional diffusion map: A noninvasive MRI biomarker for early stratification of clinical brain tumor response. *Proc Natl Acad Sci USA* 2005; 102: 5524-5529.
15. Tsien C, Galbán CJ, Chenevert TL, Johnson TD, Hamstra DA, Sundgren PC, Junck L, Meyer CR, Rehemtulla A, Lawrence T, Ross BD. Parametric response map as an imaging biomarker to distinguish progression from pseudoprogression in high-grade glioma. *J Clin Oncol* 2010; 28: 2293-399.
16. Chitphakdithai N, Chian VL, Duncan JS. Non-rigid registration of longitudinal brain tumor treatment MRI. *Conf Pric IEEE Eng Med Biol Soc* 2011; 2011: 4893-4896.
17. Chitphakdithai N, Vives KP, Duncan JS. Registration of brain resection MRI with intensity and location priors. *Proceedings of the IEEE International Symposium on Biomedical Imaging: From Nano to Macro*, Chicago, USA, 2011; 1520-1523.
18. Liu Y, Yao C, Zhou LF, Chrisochoides N. A point based non-rigid registration for tumor resection using IMRI. *Proceddings of the IEEE International Symposium on Biomedical Imaging: From Nano to Macro*, Rotterdam, the Netherlands, 2010; 1217-1220.
19. Nithiananthan S, Schafer S, Mirota DJ, Stayman JW, Zbijewski W, Reh DD, Gallia GL, Siewerdsen JH. Extra-dimensional Demons: A method for incorporating missing tissue in deformable image registration. *Med Phys* 2012; 39: 5718-5731.
20. Ding S, Miga M, Noble JH, Cao NA, Dumpuri P, Thompson RC, Dawant BM. Semiautomatic registration of pre- and postbrain tumor resection laser range data: Methods and validation. *IEEE Trans Biomed Eng* 2009; 56: 770-780.

21. Rivaz H, Chen SJS, Collins DL. Automatic deformable MR-ultrasound registration for image-guided neurosurgery. *IEEE Trans Med Imaging* 2015; 34: 366-380.
22. Risholm P, Samset E, Talos IF, Wells W. A non-rigid registration framework that accommodates resection and retraction. *Inf Process Med Imaging* 2009; 21: 447-458.
23. Smith SM. Fast robust automated brain extraction. *Hum Brain Mapp* 2002; 17: 143-155.
24. Zhang Y, Brady M, Smith S. Segmentation of brain MR images through a hidden markov random field model and the expectation-maximization algorithm. *IEEE Trans Med Imaging* 2001; 20: 45-57.
25. Wang Z, Bovik AC, Sheikh HR, Simoncelli EP. Image qualifty assessment: From error visibility to structural similarity. *IEEE Trans Image Process* 2004; 13: 600-612.
26. Cohen DS, Lustgarten JH, Miller E, Khandji AG, Goodman RR. Effects of coregistration of MR to CT images on MR stereotactic accuracy. *J. Neurosurg* 1995; 82: 772-779.
27. Schucht P, Knittel S, Slotboom J, Seidel K, Murek M, Jilch A, Raabe A, BeckJ. 5-ALA complete resections go beyond MR contrast enhancement: shift corrected volumetric analysis of the extent of resection in surgery for glioblastoma. Acta Neurochi 2014; 156: 305-312

TABLE 1 – Targeted coregistration errors between pre- and post-operation

		Postoperative with preoperative				
		SAC	**FLIRT**	**FNIRT**	***SAC versus FLIRT***	***SAC versus FNIRT***
		mean (range)	**mean (range)**	**mean (range)**	***P*-value**	***P*-value**
Central	**x**	3.0 (0.3-10.6)	3.3 (0.3-10.6)	7.0 (0.1-46.6)	0.242	0.023*
tumor/	**y**	2.5 (0.1-7.4)	2.8 (0.1-8.3)	4.8 (0.2-28.2)	0.256	0.031*
cavity	**z**	2.6 (0.0-8.1)	2.7 (0.1-10.3)	5.2 (0.4-57.0)	0.758	0.003*
	vector	5.3 (1.5-11.1)	5.7 (1.3-15.2)	11.6 (0.3-16.9)	0.099	0.002*
Cerebral	**x**	0.5 (0.0-1.0)	0.7 (0.0-5.0)	0.6 (0.0-4.0)	0.166	0.305
aqueduct	**y**	0.8 (0.0-3.0)	1.2 (0.0-5.0)	2.7 (0.0-6.0)	0.051	<0.001*
	vector	1.1 (0.0-3.2)	1.6 (0.0-5.4)	2.9 (0.0-6.1)	0.015*	<0.001*
Septum	**x**	0.8 (0.0-4.0)	1.3 (0.0-9.0)	1.2 (0.0-9.0)	0.132	0.280
pellucidum	**y**	1.3 (0.0-4.0)	2.0 (1.0-8.0)	3.6 (1.0-7.0)	0.029*	<0.001*
	vector	1.8 (0.0-4.5)	2.6 (0.0-9.1)	4.0 (2.7-108.5)	0.021*	<0.001*
Third	**y**	0.4 (0.0-1.0)	2.2 (0.0-18.0)	1.7 (0.0-6.0)	<0.001*	<0.001*
ventricle	**z**	1.2 (0.0-4.0)	1.9 (0.0-14.0)	3.9 (0.0-12.0)	0.043*	<0.001*
	vector	1.3 (0.0-4.1)	3.3 (0.0-18.0)	4.5 (1.0-12.4)	<0.001*	<0.001*

Targeted registration error are provided with the deviations (mm) of the anatomical landmarks coordinates to the reference images after coregistration of the postoperative to the preoperative scan and the preoperative with the recurrence scan by using the semi-automatic non-linear coregistration (SAC), linear (FLIRT) and default non-linear (FNIRT) coregistration. An * indicates statistical significance.

TABLE 2 – Targeted coregistration errors between pre-operation and recurrence

		Recurrence with preoperative				
		SAC mean (range)	**FLIRT mean (range)**	**FNIRT mean (range)**	**SAC versus FLIRT P-value**	**SAC versus FNIRT P-value**
Central tumor/ cavity	**x**	5.0 (0.2-15.9)	5.6 (0.3-16.3)	9.9 (0.4-73.7)	0.204	0.131
	y	4.0 (0.3-16.4)	3.0 (0.3-8.6)	13.6 (0.5-13.1)	0.247	0.226
	z	5.0 (0.5-15.1)	4.2 (0.1-13.2)	11.5 (0.3-29.5)	0.297	0.008*
	vector	9.1 (0.9-20.2)	10.0 (0.9-24.4)	23.3 (2.7-108.5)	0.875	0.102
Cerebral aqueduct	**x**	1.2 (0.0-5.0)	1.3 (0.0-4.0)	0.8 (0.0-6.0)	0.822	0.280
	y	1.3 (0.0-3.0)	2.1 (0.0-5.0)	2.3 (0.0-8.0)	0.004*	0.032*
	vector	2.0 (0.0-5.8)	2.8 (0.0-5.0)	2.7 (0.0-8.2)	0.016*	0.124
Septum pellucidum	**x**	2.8 (0.0-12.0)	3.3 (0.0-14.0)	2.0 (0.0-19.0)	0.2132	0.188
	y	2.8 (0.0-15.0)	2.8 (0.0-16.0)	3.0 (0.0-17.0)	1.0000	0.779
	vector	4.3 (1.0-19.0)	4.6 (0.0-20.6)	4.1 (0.0-10.2)	0.7280	0.782
Third ventricle	**y**	0.6 (0.0-3.0)	3.0 (0.0-16.0)	3.1 (0.0-11.0)	0.0010*	0.001*
	z	2.6 (0.0-9.0)	2.5 (0.0-13.0)	3.1 (0.0-16.0)	0.8898	0.466
	vector	2.7 (0.0-9.1)	4.6 (1.0-16.0)	5.1 (0.0-16.5)	0.0112*	0.006*

Targeted registration error are provided with the deviations (mm) of the anatomical landmarks coordinates to the reference images after coregistration of the recurrence to the preoperative scan and the preoperative with the recurrence scan by using the semi-automatic non-linear coregistration (SAC), linear (FLIRT) and default non-linear (FNIRT) coregistration. An * indicates statistical significance.

FIGURE 1 - Co.-registration steps.

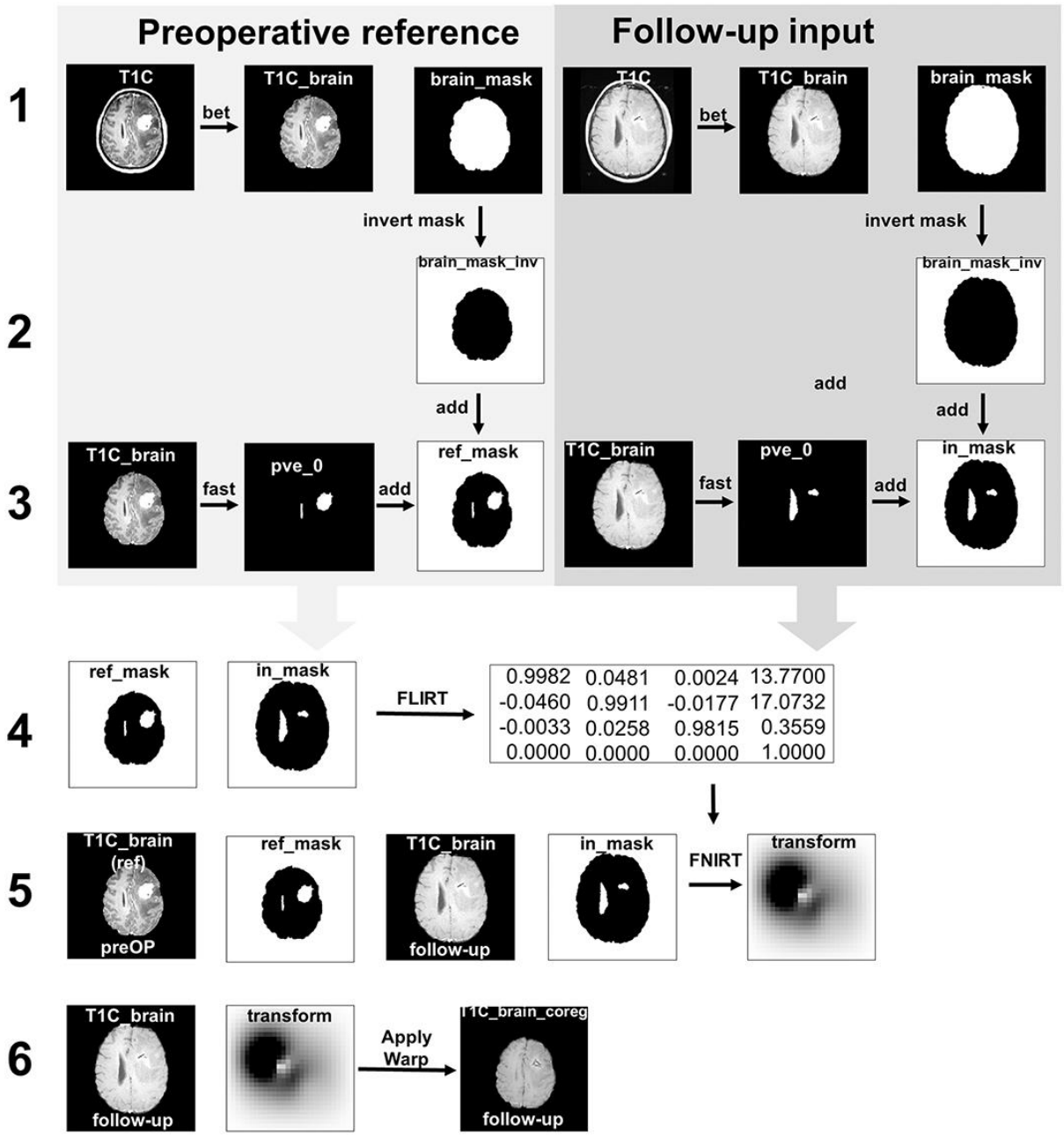

Steps for the semi-automatic co-registration of the follow-up image with the preoperative reference image. The numbers of the steps and filenames correspond to the text in Supporting information. The corresponding code can also be found in the text of Supporting information.

FIGURE 2 - Targeted registration errors.

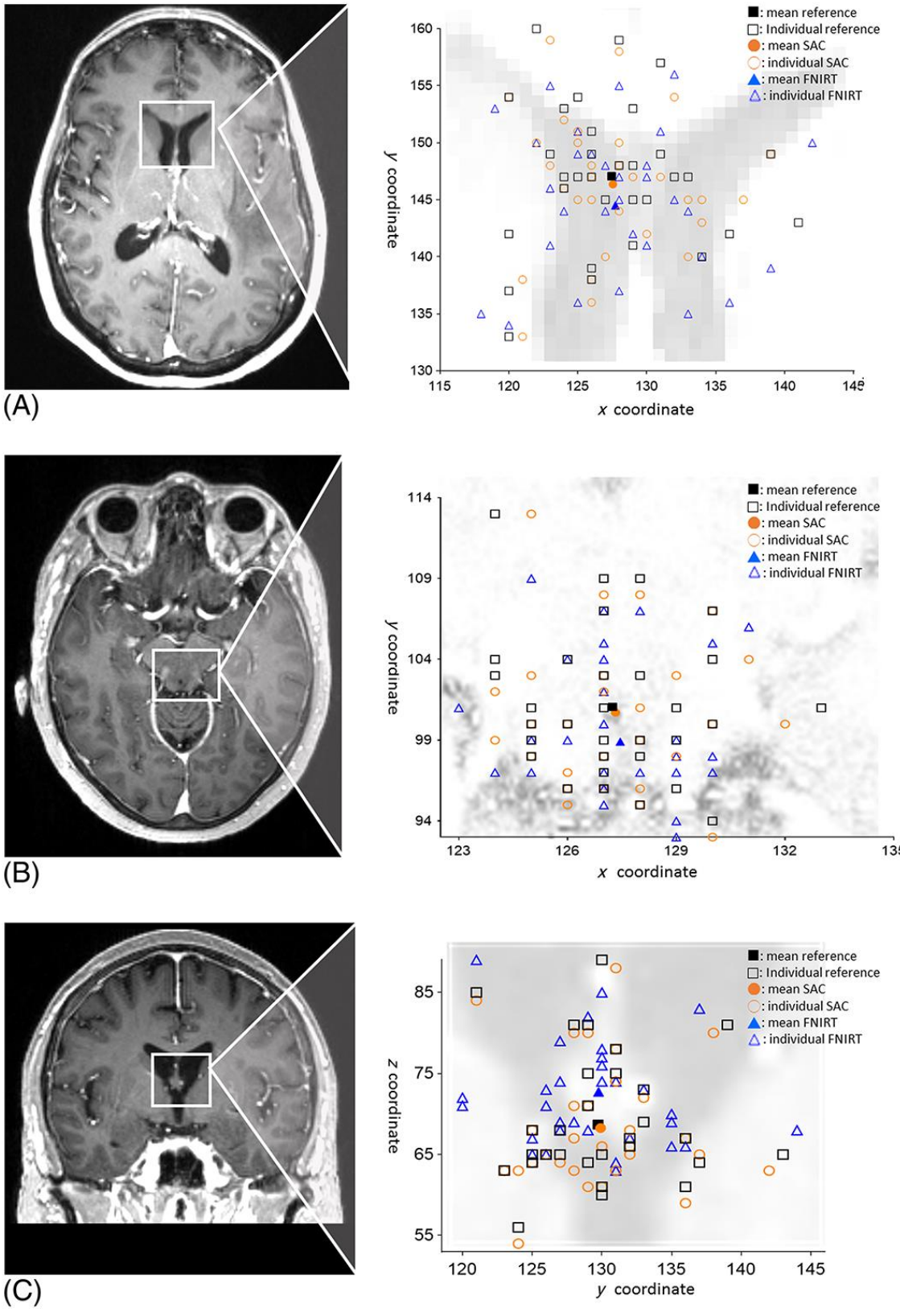

Targeted registration errors are shown for the septum pellucidum in axial view (A), cerebral aqueduct in axial view (B) and the top of the third ventricle (C). Images on the

left show individual cases to illustrate the locations of the targets and the graphs on the right correspond to the whole patient set. Squares indicate coordinates for the presurgical MRI. The group mean is indicated by a filled square (■) and individual patients by open squares (□). Circles indicate the co-registered image differences after semi-automatic non-linear co-registration (SAC) of postoperative and preoperative images. The group mean is indicated by a filled circle (●) and individual patients are indicated by open circles (○). Triangles indicate the co-registered image difference after FNIRT (FMRIB's Non-Linear Image Registration Tool) non-linear co-registration of postoperative and preoperative images. The group mean is indicated by a filled triangle (▲) and individual patients are indicated by open triangles (Δ).

FIGURE 3 - Mean three-dimensional (3D) group structural similarity for co-registration.

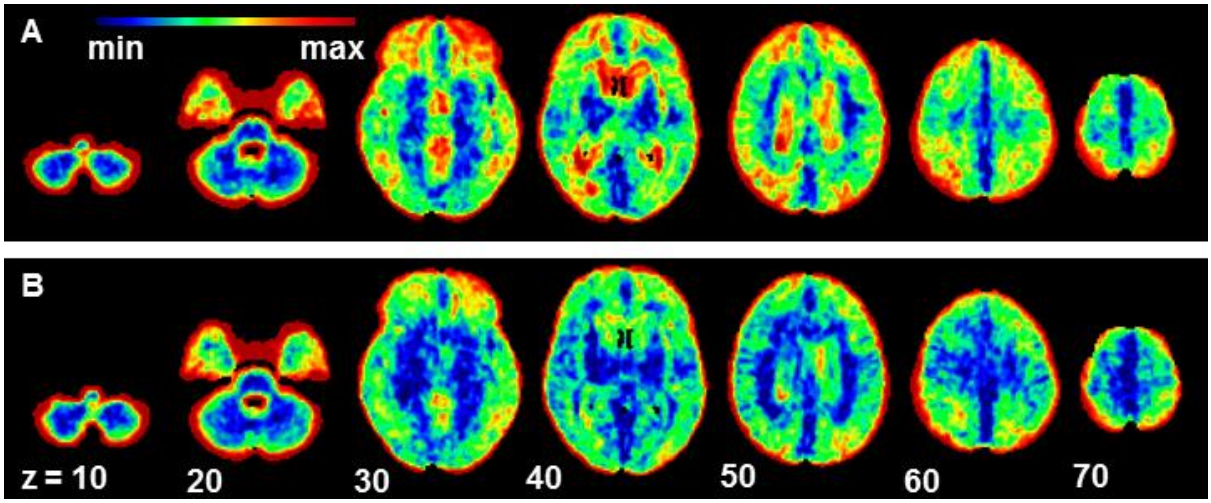

Mean three-dimensional (3D) group structural similarity for co-registration. The group mean 3D structural similarity of all 32 cases is shown for the direct postoperative MRI (A) and later follow-up MRI at the time point of tumor recurrence (B), both co-registered to the preoperative MRI. Values indicate the relative structural similarity between the co-registered and original preoperative scans for the group mean, with higher values indicating a greater similarity between the images being compared. The color bar shows the degree of similarity from totally identical (max, red) to 0% similar (min, black).

FIGURE 4 - Example of preoperative, direct postoperative and recurrence MRI co-registration.

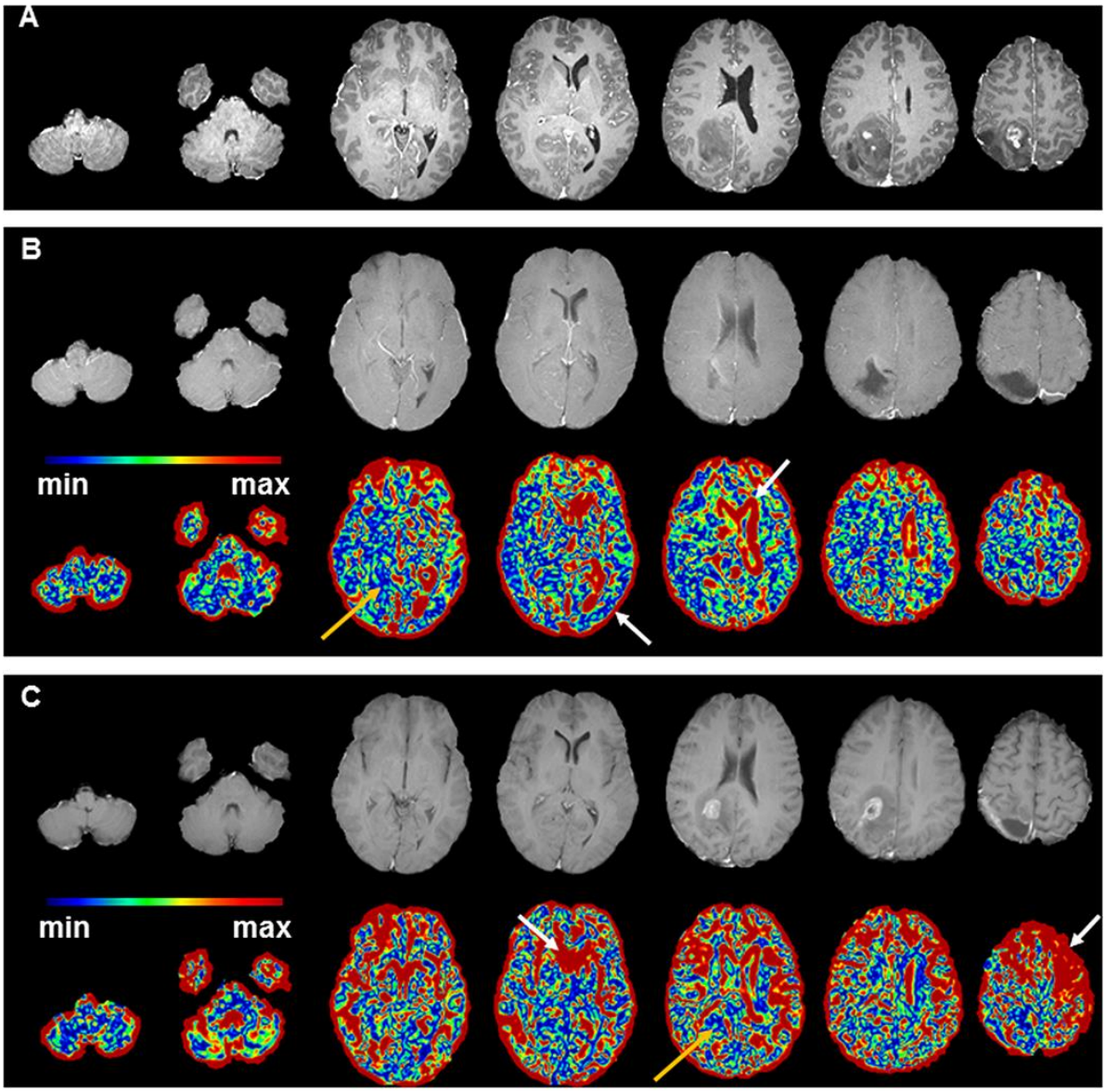

An example of a representative patient with glioblastoma. The preoperative reference scan (A) is compared with the co-registered postoperative scan (B) and recurrence scan (C). The color maps show the similarity between different time points, with red indicating a higher and blue indicating a lower similarity index. The color bar shows the degree of similarity from totally identical (max, red) to 0% similar (min, black). These comparisons demonstrate a good performance of the semi-automatic co-registration method, especially in the peripheral area and ventricle area (white arrow), whereas lower performance is observed in the brain parenchyma and tumor area (brown arrow).

FIGURE 5 - Examples of the two-stage semi-automatic non-linear co-registration.

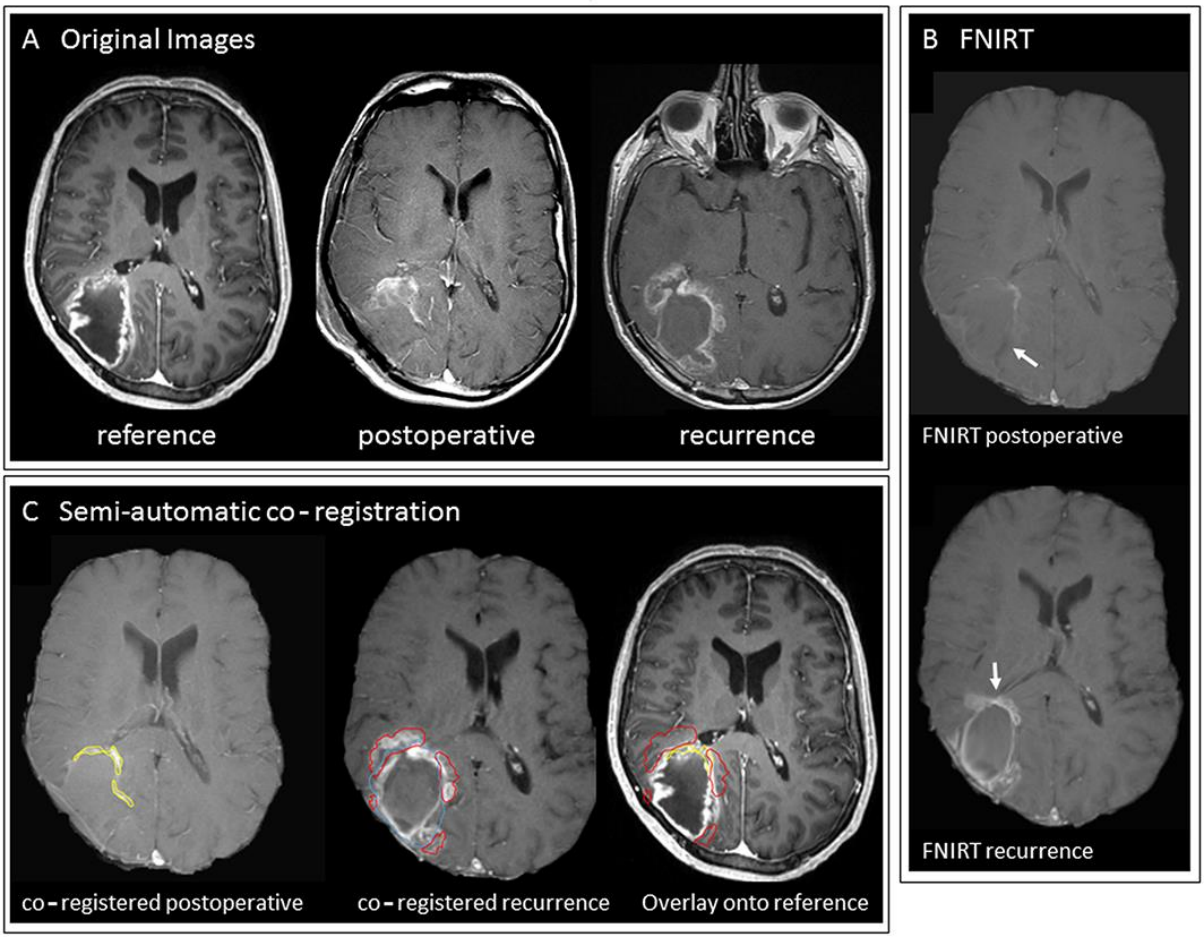

Without co-registration, the postoperative and recurrence images are difficult to compare with the preoperative reference image (A). With standard FNIRT (FMRIB's Non-Linear Image Registration Tool) co-registration (B), although the gross brain positions are realigned in both postoperative and recurrence images, regional torsion, especially around the lesion (white arrow), may occur. After semi-automatic co-registration (C), postoperative residual regions (C, left, yellow outline) and recurrence regions (C, middle, red outline) can be fitted with the preoperative reference image (C, right).